


Article

A Framework Using Open-Source Software for Land Use Prediction and Climate Data Time Series Analysis in a Protected Area of Portugal: Alvão Natural Park

Saulo Folharini * , António Vieira , António Bento-Gonçalves , Sara Silva , Tiago Marques and Jorge Novais

Communication and Society Research Centre, Department of Geography, University of Minho, 4810-058 Guimarães, Portugal

* Correspondence: sfolharini@gmail.com or b12894@ics.uminho.pt

Abstract: Changes in land use and land cover (LULC) in protected areas can lead to an ecological imbalance in these territories. Temporal monitoring and predictive modeling are valuable tools for making decisions about conserving these areas and planning actions to reduce the pressure caused by activities such as agriculture. This study accordingly developed an LULC analysis framework based on open-source software (QGIS and R language) and predictive methodology using artificial neural networks in the Alvão Natural Park (PNA), a protected area in northern Portugal. The results show that in 2041, Agriculture and Open Space/Non-vegetation classes will evidence the greatest decrease, while Forest and Bushes will have expanded the most. Spatially, the areas to the west and northeast of the protected area will experience the most significant changes. The relationship of land use classes with data from the climate model HadGEM3-GC31-LL (CMIP6) utilizing scenarios RCP 4.5 and 8.5 demonstrates how through the period 2041–2060 there is a tendency for increased precipitation, which when combined with the dynamics of a retraction in classes such as agriculture, favors the advancement of natural classes such as bushes and forest; however, the subsequent climate data period (2061–2080) projects a decrease in precipitation volumes and an increase in the minimum and maximum temperatures, defining a new pattern with an extension of the period of drought and precipitation being concentrated in a short period of the year, which may result in a greater recurrence of extreme events, such as prolonged droughts that result in water shortages and fires.

Keywords: LULC; Molsuce plugin; WordClim; OpenLand

Citation: Folharini, S.; Vieira, A.; Bento-Gonçalves, A.; Silva, S.; Marques, T.; Novais, J. A Framework Using Open-Source Software for Land Use Prediction and Climate Data Time Series Analysis in a Protected Area of Portugal: Alvão Natural Park. *Land* **2023**, *12*, 1302. <https://doi.org/10.3390/land12071302>

Academic Editor: Nir Krakauer

Received: 19 May 2023

Revised: 16 June 2023

Accepted: 26 June 2023

Published: 28 June 2023



Copyright: © 2023 by the authors. Licensee MDPI, Basel, Switzerland. This article is an open access article distributed under the terms and conditions of the Creative Commons Attribution (CC BY) license (<https://creativecommons.org/licenses/by/4.0/>).

1. Introduction

Among the Sustainable Development Goals (SDGs), environmental sustainability is a key theme that emphasizes the preservation of natural resources at levels that will not compromise future generations. The mitigation of climate change is directly linked to the preservation of ecosystems through Protected Areas (PAs), which guarantee the balance of natural systems [1,2]. PAs territories play a crucial role in ensuring the sustainability promoted by the SDGs. They possess natural, ecological, and cultural values that must be preserved [3].

The earliest Protected Areas (PAs) were established to preserve iconic landscapes and species, such the first National Park in the United States, Yellowstone. Currently, PAs play a variety of roles, including developing tourism-related activities, conserving biodiversity, achieving social and community goals, and providing ecosystem services. If PAs had not been developed throughout the twentieth century, then the current biodiversity crisis would be worse. With insufficient funding for the management of PAs, a countries' efforts to address the current biodiversity issue will fall short of what was outlined in the Convention on Biological Diversity (CBD) strategic plan for 2020 [4,5].

Climate change makes conservation initiatives harder. The relevance and concern around the conservation of PAs grows owing to the pressure on natural ecosystems brought

on by global population growth and resource usage. In addition to supplying necessities such as water, food, and pharmaceuticals derived from native species, PAs are also playing an increasingly significant role in absorbing carbon and helping mitigate climate change's consequences [4].

According to Melillo et al., PAs on Earth yearly capture 0.5 Pg C, approximately one-fifth of the carbon stored by terrestrial ecosystems. They predict that in 2100, due to changes in usage and coverage, this amount will decrease to 0.3 Pg C [6].

PAs experience changes in Land Use and Land Cover (LULC), which diminish their resilience and affect the availability of ecosystem services, failing to meet their protection and conservation objectives. This scenario is observed in various PAs worldwide, including Brazil [7–9], Ecuador [10], the African continent [11,12], and the European continent [13,14].

LULC monitoring is essential for analyzing temporal patterns and for identifying the variations responsible for changes in the use and coverage of a location. Scientific research in the field of LULC is currently developing methodologies based on artificial neural networks (ANN) for predicting use and coverage, using a database with a high spatial resolution that makes it possible to identify patterns of changes at local levels, which can help territorial governance actions to mitigate the effects resulting from the lack of territorial planning and to plan actions to mitigate climate change resulting from the loss of biodiversity [15–18].

ANN are self-learning computer models used to recognize patterns. In the LULC modeling, the ANN relates past and future land-use changes, training itself based on land use maps from different years, while recognizing and reproducing patterns of land use categories [19].

The application of spatial prediction using ANN in PAs helps to understand whether there were changes in LULC in areas where the preservation and conservation of the natural environment must prevail to guarantee the functioning of ecosystems and thus the provision of ecosystem services such as water supply, carbon stock, and retention of sediments that result in the loss of biodiversity [20,21].

The joint analysis of LULC data and climate models resulting from the Coupled Model Intercomparison Project Phase 6 (CMIP6) provides an analysis to identify whether the patterns identified in the LULC predictive model are valid when related to climate models that provide future climate patterns, with variables that are important for understanding the possible dynamics of retraction or increase of LULC [22–24]. Guo et al. [25] examined the associations between LULC and RCP 4.5 and 8.5 climatic scenarios, showing how RCP scenarios may correspond to different LULC changing trends and affect the supply of ecosystem services in the future. Expanding forest areas in the Val d'Aran region of the Pyrenees, Spain, may assist for reducing susceptibility to landslides in places with a history of these events, according to Hürlimann et al. [26] who examined the impacts of LULC changes and precipitation on landslide susceptibility. Accordingly, this study uses only open source software, namely QGIS (plugin MLUSCE) and R language to develop an LULC predictive analysis framework for the year 2041 in the Alvão Natural Park (PNA) in northern Portugal, and the relationship between this change and the climate conditions, based on data from the HadGEM3-GC31-LL (CMIP6) model [27] utilizing the Representative Concentration Pathways (RCP) 4.5 and 8.5 scenarios, referring to the minimum temperature, maximum temperature, and precipitation variables provided by the WordClim portal [22] for the historical periods 2021–2040, 2041–2060, and 2061–2080 in 30-s resolution.

With the help of this analysis, it was possible to develop a future scenario for the climate in each LULC class. This relationship can aid in the formulation of public policies to protect the PNA's biodiversity in a scenario of climate change where the occurrence of extreme events, such as wildfires, are becoming more frequent and degrading the biodiversity of PNAs.

2. Materials and Methods

The LULC modeling steps of the PNA were divided between obtaining and pre-processing the data and modeling using the Molusce plugin, available in QGIS, version 2.18. Figure 1 shows a flowchart with the processing steps.

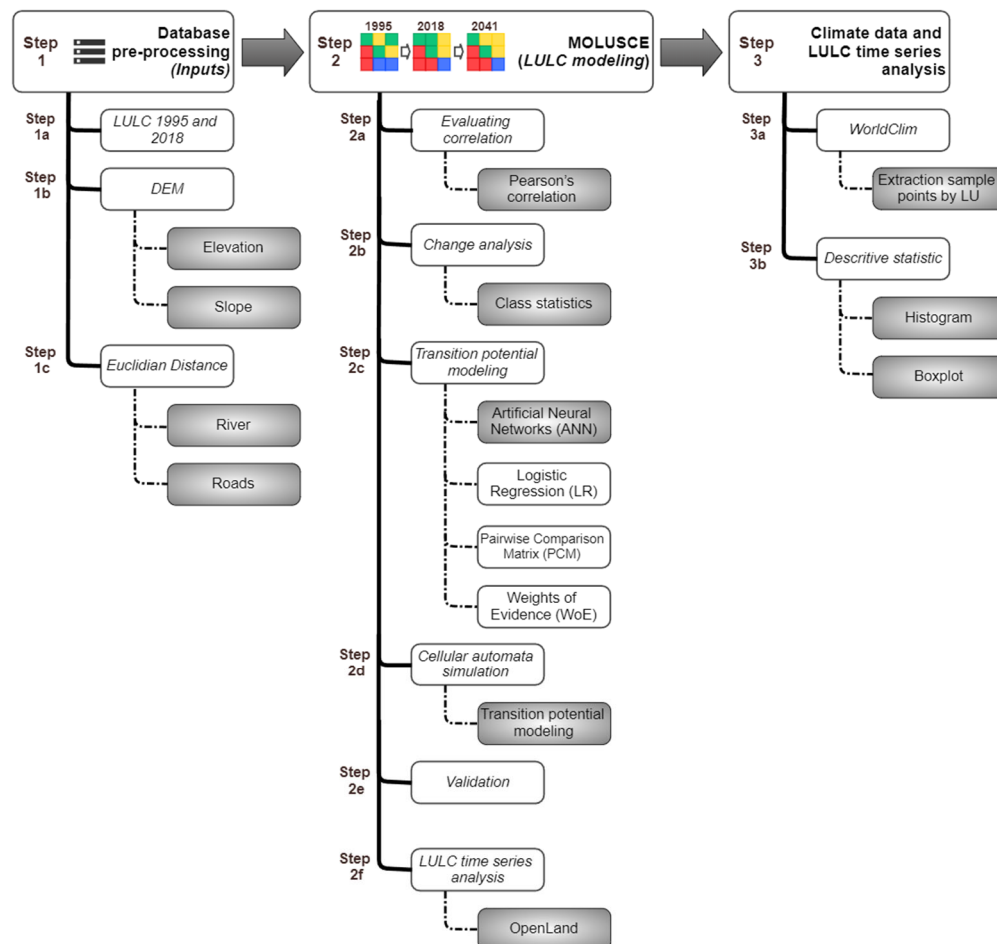


Figure 1. Methodology steps.

2.1. Inputs

The Land Use and Occupation Charters (COS, Portuguese acronym) of 1995 and 2018 have been made available by the Directorate-General for Territory (DGT). COS provides land use and coverage cartography with a minimum cartographic unit defined as 1 ha. To maintain consistency between the years 1995 and 2018, we used the level 1 detail provided by COS.

In addition to the land use and land cover maps, we utilized elevation and slope data that were derived from the Digital Elevation Model (DEM) with a resolution of 25 m and the distance from rivers, which were calculated using the Euclidean Distance tool in ArcGIS using the drainage network. The DEM and drainage network were provided by the European Environment Agency (EEA). The road distance was also calculated using the Euclidean Distance tool from the National Road Network database, which was made available by the [Dados.gov](https://dados.gov.pt) portal.

2.2. Evaluating Correlation

The correlation analysis between the model's input variables is conducted at the LULC modeling first step. Three correlation methods are covered in this module: Joint Information Uncertainty, Cramer's coefficient, and Pearson's correlation. In investigations

connecting LULC with other environmental factors, the Pearson's correlation coefficient with statistical significance at the $p < 0.05$ level approach is frequently used [28–30].

2.3. Change Analysis

The space-time change of the Land Use Cover (LUC) is estimated in the change analysis step, with the class statistics showing the initial and final areas of the LUC and the calculation of the transition matrix showing the proportion of pixels changed from one LUC to another. It is also in this step that the change map, raster with changes in classes, is performed.

2.4. Transition Potential Modeling

The transition potential between LULC can be modeled using four methods: Artificial Neural Networks (ANN), Logistic Regression (LR), Pairwise Comparison Matrix (PCM), and Weights of Evidence (WoE).

The ANN method is widely used in LULC models, as demonstrated in previous studies such as [31–35]. In our study, we defined five input parameters:

- Neighborhood, that defines the number of pixels neighboring to the central pixel. For this analysis, we set the size to 1, which is equivalent to a 3×3 matrix.
- Learning rate, momentum, and maximum iterations which define the model learning parameters. Among these parameters, the learning rate determines the speed of the model learning; large rates enable fast but unstable learning that results in spikes in the graph, whereas small rates provide stable but slow learning. We set the values to 0.001 for the learning rate, 100 for maximum iterations, and 0.005 for momentum.
- Hidden layers, which is a list of numbers ($n_1, n_2, n_3 \dots, n_k$), where n_1 is the number of neurons in the first hidden layer, n_2 is the number of neurons in the second, and so on up to n_k , which is the number of neurons in the last hidden layer. For this research, we set the value to 10 for the hidden layers.

After processing, three numerical results are presented: the minimum validation overall error, which indicates the minimum error found in the validation of the set of samples; Δ overall accuracy, which shows the difference between the found error and the actual error; and the current validation kappa, which sets the kappa value.

Molusce also offers the options of using Logistic Regression (LR), Pairwise Comparison Matrix (PCM), and Weights of Evidence (WoE) methods. However, all three methods require user intervention to define parameters, intervals, samples, and values, thus requiring human interpretation in the process, which may affect the results of the process. Therefore, considering the extensive literature on the application of ANN in LULC models, we consider the use of this method as the most appropriate option [36–40].

2.5. Cellular Automata Simulation and Validation

In the Cellular Automata Simulation step, it is possible to produce the LULC simulation map derived from the result of the Transition potential modeling step. In this step, we set the year 2041 to maintain the proportion between the dates of the entry use and coverage maps (t_0 and t_1).

Then, the simulation results were validated. For this, it is necessary to load the reference use and coverage, and we used the classification of 2018 and the simulated use and coverage of 2041. We define the value of 5 iterations. After validation, the values of % of correctness, kappa (overall), kappa (histo), and kappa (loc) can be calculated.

2.6. LULC Time Series Analysis

The time series analysis of LULC was conducted using the R language with the OpenLand package developed by Exavier and Zeilhofer [41]. This package provides several functions for visualization and analysis from LUC to intensity analysis that use cross-tabulation matrices. In this process, the deviation between the observed change intensity and the intensity of uniform change is evaluated at three levels: (1) indication

of the size and rate of change over time intervals; (2) category level analysis of the size and intensity of losses and gross gains in categories in each time interval; and (3) the transition level, which determines the intensity and size in each category in the analyzed time interval.

In this study, we used the analysis functions of net and gross gains and losses of the use classes to create a bar chart, an elaborate Sankey chart that provides the visualization of the transitions of the use classes in all of the time series, and an analysis of accumulated changes in pixels, where the results are presented in percentage of changes per transition class, indicating the number of changes in the total time interval analyzed.

2.7. Climate Data and LULC Time Series Analysis

The climate data analyzed are projections from the Coupled Model Intercomparison Project (CMIP6), which underwent calibration (bias correction) and a downscaling process and were made available by the WorldClim platform, version 2.1. Monthly data from the global climate model (GCM) HadGEM3-GC31-LL were analyzed [23,27,42], representing Representative Concentration Pathways (RCP) scenarios 4.5 and 8.5 for the variables of minimum temperature, maximum temperature, and precipitation, available as average values for the periods of historical climate data, 2021–2040, 2041–2060, and 2061–2080 at a resolution of 30 s. Data access was performed using the R language and the geodata package.

The raster was uploaded to ArcGIS, where a shapefile of sampling points was initially generated using the Create Fishnet tool with 7217 points spaced 100 m apart. Afterward, the Extract Multi Values to Points tool was used to extract the values of the pixels referring to the variables of minimum temperature, maximum temperature, precipitation, and land use classes for 1995, 2018, and 2041. Figure 2 and Table 1 show the number of sampling points by land use class in 1995, 2018, and 2041.

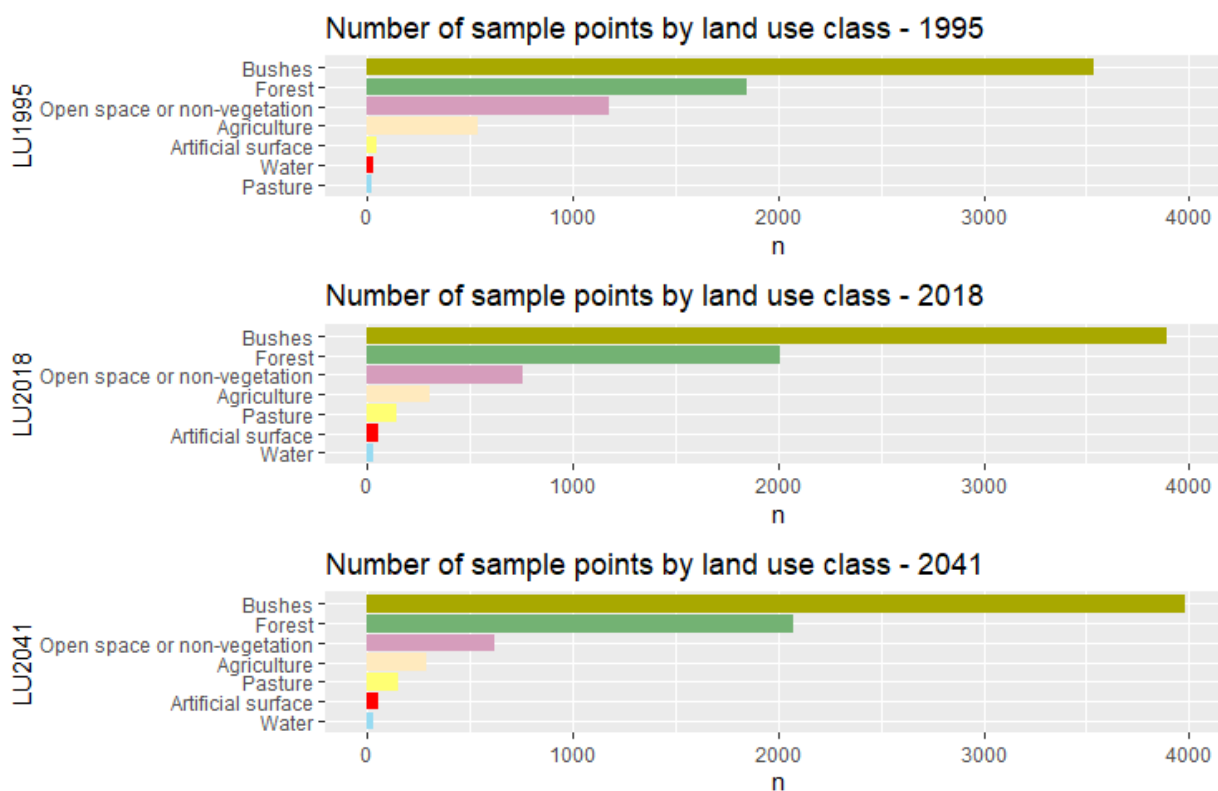


Figure 2. Sample points by land use class.

Table 1. Number of sample points by land use class.

	LU 1995	LU 2018	LU 2041
Bushes	3538	3894	3983
Forest	1846	2008	2072
Open space or non-vegetation	1183	760	624
Agriculture	542	310	289
Artificial surface	47	146	156
Water	37	62	61
Pasture	24	37	32
Total	7217	7217	7217

Next, the shapefile files were inserted into R language, and using the ggplot2, gridExtra, dplyr, tidyverse, sf packages, a descriptive statistical analysis was carried out, creating bloxplot graphs and histograms to identify average values of minimum temperature, maximum temperature, and precipitation by class of land use in the historical and future periods 2021–2040 and 2041–2060.

3. Results

We present LULC prediction results for 2041, area tables (ha), Sankey analysis, Net and Gross gain and loss, changes in the interval 1995–2041, and climate analysis relating LULC classes with climate variables. In the Supplementary Materials, we provide additional analysis data.

3.1. LULC

Pearson’s correlation (Table 2) measured the degree of association between the explanatory variables, which can influence the expansion or retraction of LU classes.

Table 2. Evaluation correlation of variables in PNA.

	Road Distance	Slope	Elevation	River Distance
Road distance	--	−0.496	0.672	0.181
Slope		--	−0.523	−0.333
Elevation			--	0.650
River distance				--

The variables road distance and elevation (0.672), in addition to river distance and elevation (0.650) plus river distance and road distance (0.181) have a positive correlation. The variables road distance and slope (−0.496), slope and elevation (−0.523), and slope and river distance (−0.333) have a negative correlation.

The LULC with the areas (ha) of the classes is represented in Figure 3 and Table 3. The validation of the LULC model for 2041 recorded kappa 0.96.

Table 3. LULC area change (ha) in PNA.

Classes	1995	2018	2041	Difference 1995–2018	Difference 2018–2041	Difference 1995–2041
Artificial surface	45.14	58.82	57.03	13.68	−1.79	11.89
Agriculture	561.14	323.61	302.53	−237.53	−21.08	−258.61
Pasture	26.56	153.61	159.27	127.06	5.66	132.72
Forest	1864.86	2018.94	2086.70	154.08	67.76	221.84
Bushes	3526.49	3896.19	3989.86	369.70	93.67	463.37
Open space or non-vegetation	1178.73	751.74	614.95	−426.99	−136.79	−563.78
Water	35.38	35.38	28.31	0.00	−7.07	−7.07

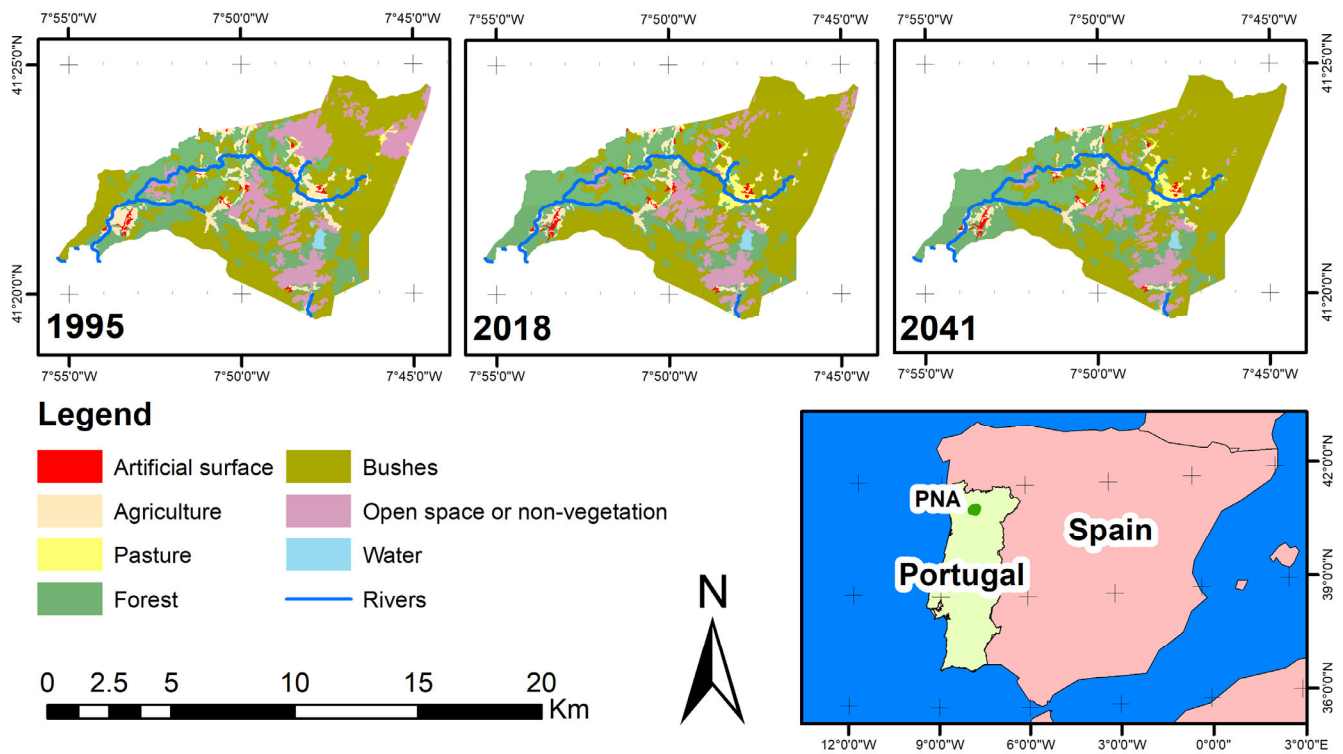


Figure 3. LULC 1995, 2018 and 2041.

Losses and gains by LULC class are identified in Figure 4.

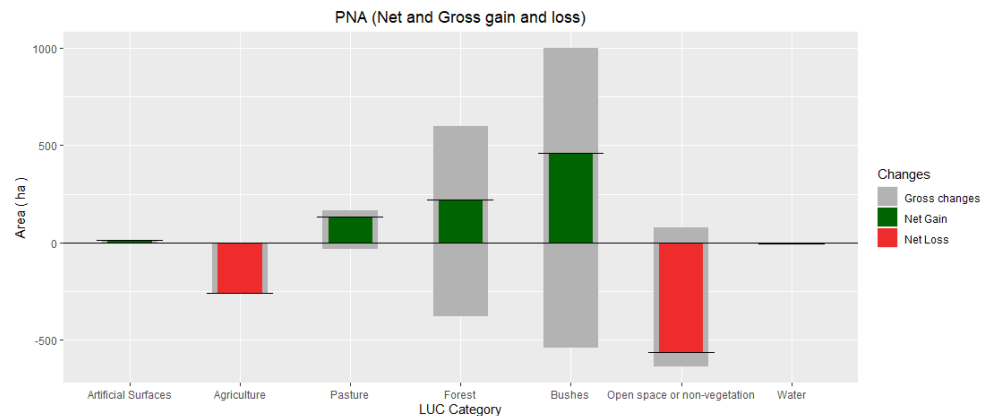


Figure 4. Net and Gross changes in the PNA.

PNA classes with a significant decrease in the area are Agriculture (−258.61 ha) and Open Space or non-vegetation (−563.78 ha), in addition to Water (−7.07 ha) which also registered a small decrease. Meanwhile, the Pasture, Forest, Bushes, and Artificial surface classes increased, respectively, by 132.72 ha, 221.84 ha, 463.37 ha, and 11.89 ha in the period 1995–2041. The changes that took place between classes are best visualized in Figure 5.

The Agriculture class (322.97 ha of permanence) was the most altered in the period 1995–2018, converting to all other classes, except Water (35.3 ha of permanence). Next were the classes Forest (1524.89 ha permanence) and Bushes (322.97 ha permanence) which became Artificial surface (1 ha and 3.98 ha), Pasture (10.7 ha and 1.77 ha), Open space or non-vegetation (20.53 ha and 50.49 ha), and between these were Bushes (308.62 ha) and Forest (381.38 ha), evidencing ecological succession. The Open space or non-vegetation class was converted into Artificial surface (0.2 ha), Forest (31.12 ha), and mainly Bushes (467.35 ha), demonstrating revegetation of areas where there was no vegetation cover.

The Pasture class was converted into Forest (4.59 ha) and mainly Bushes (19.94 ha). The Artificial surface class became Agriculture (0.04 ha).

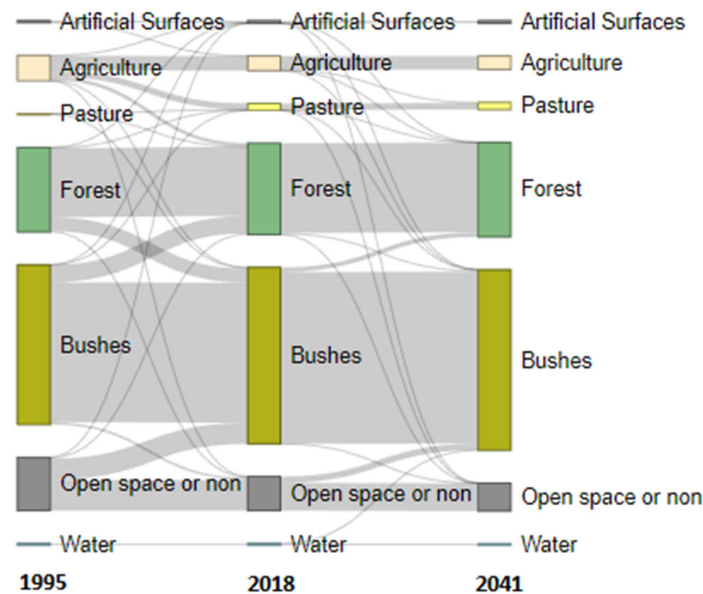


Figure 5. Sankey graphic, change between classes in the PNA.

Between 2018 and 2041, the Artificial surface class (57.11 ha of permanence) has a greater forecast of change to the Forest (0.2 ha), Bushes (8.01 ha), Open space or non-vegetation (0.54 ha), and Water (28.25 ha) classes. The Agriculture class (302.67 ha permanence) changes to Pasture (14.07 ha), Forest (3.77 ha), and Bushes (2.5 ha). The Pasture class (144.83 ha of permanence) changes to Forest (0.03 ha), Bushes (6.67 ha), and Open space or non-vegetation (1.82 ha). The Forest class (1980.92 ha permanence) changes to Bushes (36.62 ha) and Open space or non-vegetation (2.4 ha). In the Bushes class (3794.71 ha of permanence), the alteration registered is to Forest (101.51 ha) and Open space or non-vegetation (0.06 ha). Finally, Open space or non-vegetation (611.71 ha of permanence) registers a tendency to change to Bushes (140.31 ha).

The observed changes are not evenly distributed across the territory. Some locations were more altered than others and this can be seen in Figure 6:

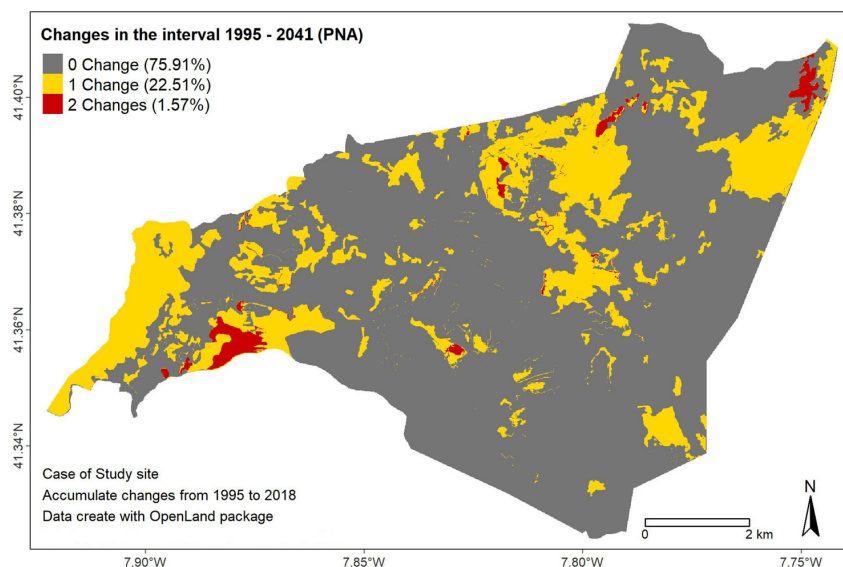


Figure 6. Changes in the interval 1995–2041 in the PNA.

The simulation indicates that the territory of the PNA will remain unchanged in 75.91% of its area, in 22.51% there will be at least one change, and in 1.57% there will be two changes. There is a concentration of two changes in the southwest and northeast regions of the PNA, while one change occurs distributed throughout the territory.

3.2. Climate Historical and Future Data by Land Use Classes in 1995, 2018, and 2041

Figure 7 shows the boxplots with historical precipitation values and RCP 4.5 and 8.5 scenarios of the sampling points by land use class in 1995, 2018, and 2041.

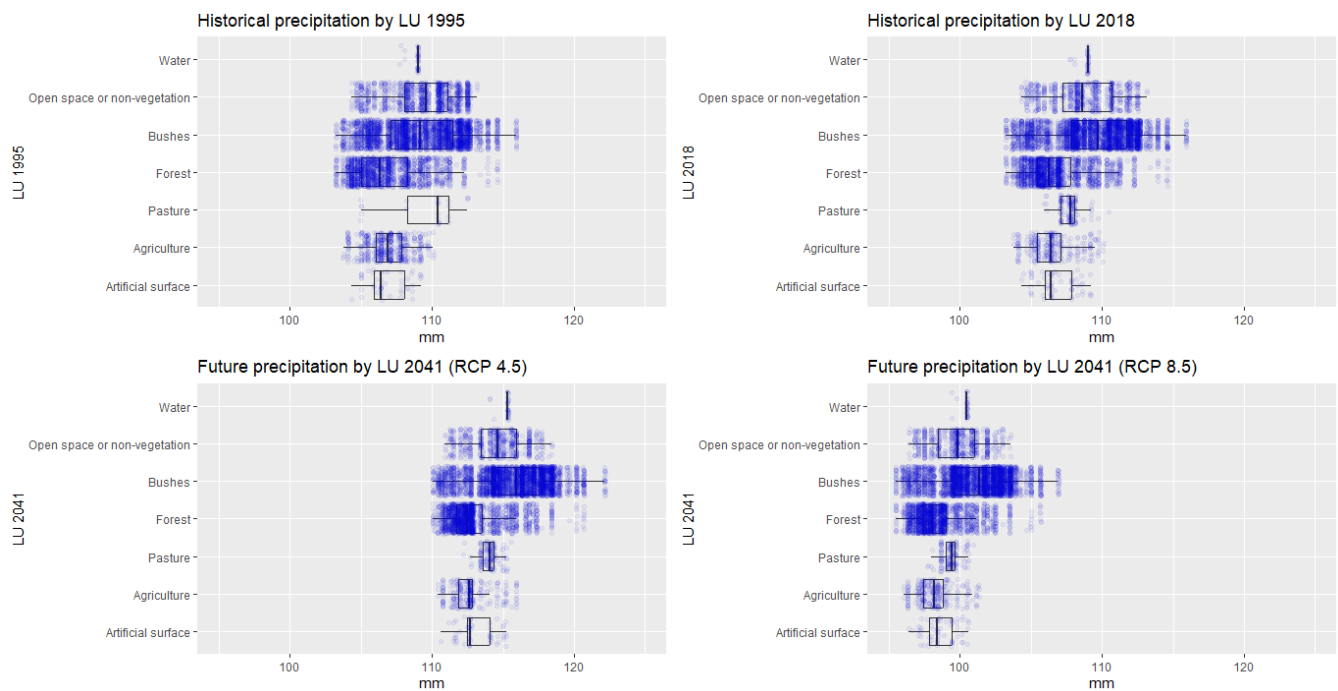


Figure 7. Historical and future (RCP 4.5 and 8.5) precipitation by LU classes.

Historical precipitation values registered a small change in volume only in the pasture class, with the minimum value increasing by 0.9 mm, the maximum value decreasing by 2 mm, and the mean decreasing by 3.1 mm in the period 1995–2018. The Pasture class recorded the largest average decrease of 1.8 mm over the historical period.

In turn, between 2018 and 2041 in the RCP 4.5 scenario, there is an increasing trend between 6.3 (Water, Pasture, and Artificial surface) and 6.9 mm (Forest and Bushes) in the minimum values of precipitation in all LULC classes. The maximum values tend to increase between 5.1 mm (Pasture) and 6.3 mm (Bushes and Water). The average values tend to range between 5.2 mm (Open space or non-vegetation) and 6.3 mm (Artificial surface and Water).

In the RCP 8.5 scenario, the minimum precipitation values tend to decrease between 7.7 mm (Forest and Bushes) and 8.38 mm (Water). The maximum precipitation values tend to decrease by 8.5 mm (Water) and 9.62 mm (Open space or non-vegetation). Mean values showed a downward trend of 8.4 mm. Between the RCP 4.5 and 8.5 models, there is an average difference in rainfall decrease between 14.45 and 14.79 mm.

Figure 8 shows the historical minimum temperature boxplots and the RCP 4.5 and 8.5 scenarios.

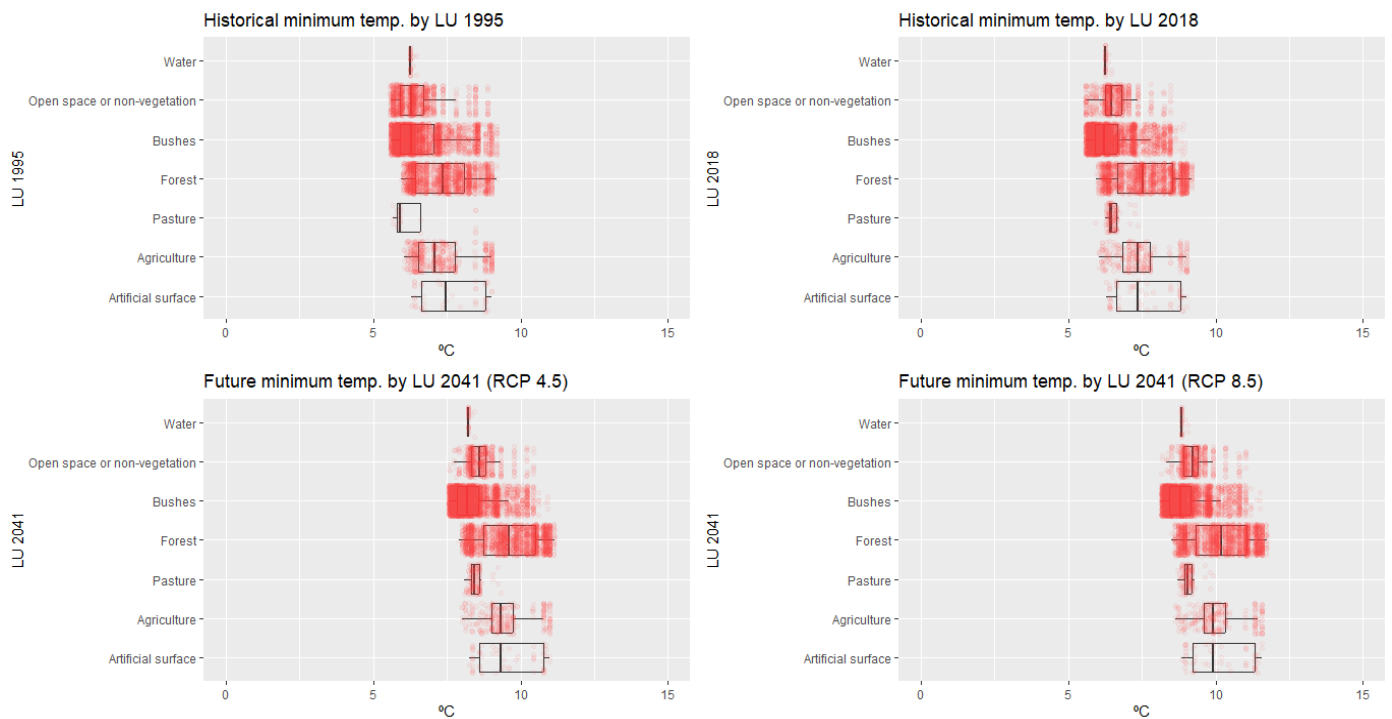


Figure 8. Historical and future (RCP 4.5 and 8.5) minimum temperature by LU classes.

Historical values (1995–2018) of minimum temperature register stability, with greater variation in the pasture class, which decreased by 1 °C. In the RCP 4.5 scenario, the most significant increase registered was in the pasture class with an increase of 2.6 °C, while the other LULC classes registered an increase between 1.96 and 1.98 °C. In the RCP 8.5 scenario, the highest minimum temperature increase tends to be an average increase of 2.59 °C, with the Agriculture class recording the highest average increase of 2.63 °C concerning historical data (1975–2018).

Figure 9 shows historical values and scenarios RCP 4.5 and 8.5 of maximum temperature.

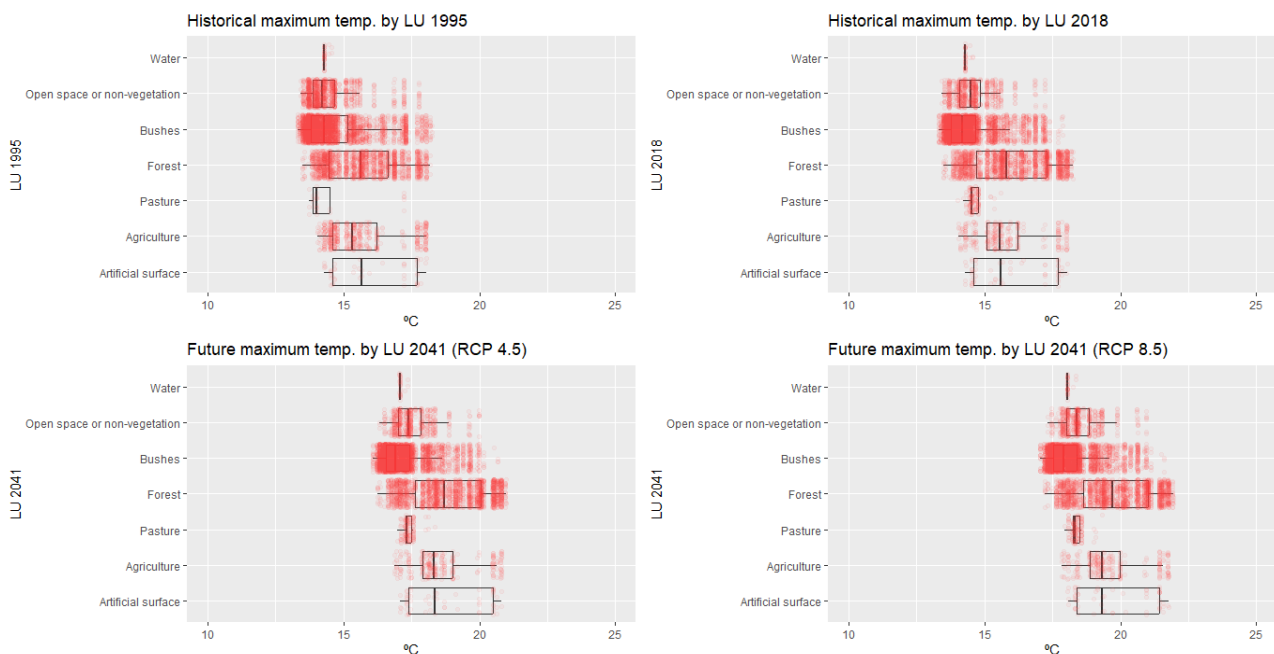


Figure 9. Historical and future (RCP 4.5 and 8.5) maximum temperature by LU classes.

Historical values (1995–2018) of maximum temperature recorded a decrease of 1.63 °C (Pasture) and −1 °C (Water), with an average increase of 0.09 °C, representing the stability of climatic conditions in the period. In the RCP 4.5 scenario, the maximum temperature of all LULC classes registers an average increase trend of 2.82 °C. In turn, the RCP 8.5 scenario registers an average increase of 3.8 °C in all LULC classes.

4. Discussion

LULC modeling is a technique that is currently used in various land management studies. As protected areas (PAs) are environments that are susceptible to external conditions resulting from human occupation, their management plan must include proposals for predictive modeling of LULC to propose actions for control and management of the territory.

In Portugal, the model adopted is the occupation permit, with activities that were already installed in the territory that became a PA and now have their regulation. In addition to this characteristic in the management of its PAs, since the 1960s the country has experienced a process of abandonment of the interior, with a diversified migration process that takes place from the interior to large cities in the country, such as Porto and Lisbon, in addition to migration to other countries, mainly in Europe [43,44].

It is observed in the 2041 LULC scenario that the migration process continues in practice, with the tendency of increasing Forests, replacing Bushes, and decreasing agricultural areas. The LULC scenario generated by the QGIS plugin Molusce, achieved satisfactory results, with Kappa 0.96. The continuity of the analysis with the Open-Land package allowed a temporal analysis in graphs and maps identifying the trend of LULC variation. The use of these two open-source tools together enabled a low-cost analysis using methods already validated by land science, such as Artificial Neural Networks and cellular automata simulation.

Historically, the PNA has been predominantly occupied by small urban centers and agricultural activities [28]. The pattern of occupation in conjunction with the limits imposed on the type of activity that can be carried out in these areas aims to guarantee the balance of ecosystems. In this context, the results indicate that from 1995 to 2041, the Forest and Agriculture classes register changes. The Forest class is forecasted to increase by 3% and the Agriculture class is forecasted to retract by −3.5%. Changes in these two classes demonstrate the tendency over time for agricultural activity to cease to be a viable economic activity in these areas, thus facilitating the process of forest restoration.

The Bushes class tends to increase by 6.3%, while the Open space or non-vegetation class registers a tendency to decrease by −7.7%. These alterations are related to a change in areas without vegetation and with low vegetation in areas with arboreal vegetation, according to the dynamics of the place which may also be influenced by the implementation of silviculture activities.

In the Artificial surface class, even with an increase of 11.89 ha between 1995 and 2041, in the period from 2018 to 2041, the decrease of 1.79 ha indicates stability in the growth of inhabited areas in the PNA. This factor can be related to the continuity of the process of migration from the interior to larger centers, in process namely deruralization and litoralisation [45], which are characteristics of the population dynamics in Portugal.

To Calix [45], the northwest region of Portugal is continuously occupied with different densities, the Porto's metropolitan conurbation operating as its primary hub. Here, the industrial and logistical sectors are concentrated, along with public services and equipment. Due to the quality of life and employment opportunities provided in this area, these qualities influence internal migration, worsening the rural exodus from lower-density areas and causing the interior's physical condition to decline quickly.

The exodus process seen in Portugal during the twentieth century may have been intensified by climate change and its associated environmental and social effects. Warner et al. [46] emphasize that the ability of families to migrate is affected by climate change, with an increase in the frequency of droughts being a variable more likely to induce migration due to its more long-lasting effects.

Regarding climate changes related to the dynamics of LULC, precipitation registers an increasing trend in the period from 2021 to 2040, yet reversing in the subsequent period (2061–2080), which favors, together with the migration of the population, the process of revegetation and succession with the transformation of areas of Bushes into Forest, due to the dynamics of rising temperatures, combined with a lack of action on the part of the public powers in minimizing the effects of fires, which tend to grow even worse in the area in the twenty-first century.

However, when analyzing the RCP 4.5 and 8.5 scenarios, it is observed in the RCP 4.5 scenario that average precipitation is between 110 mm and 120 mm, while in the RCP 8.5 scenario the average precipitation is around 100 mm. The consequences of a scenario with 10 mm less precipitation as a climate pattern are severe changes in the dynamics of ecosystems, such as greater evaporation of surface water, contributing to a decrease in the area of the LU class Water [47,48].

Regarding temperature, the RCP 4.5 and 8.5 scenarios indicate months with significant trends of over 1.5 °C for increases in minimum temperatures and increases in maximum temperatures of more than 2 °C in summer and autumn months. It was also observed that the minimum temperature is the most sensitive parameter, with increases that condition a new pattern of temperature variation through the period from 2061 to 2080.

The increase in temperature, added to stability in precipitation volumes through 2041–2060, and the expansion of months with higher temperatures through autumn, are characteristics that will favor greater evaporation of surface water, which may result in lower water availability for the growth of vegetation, making it more susceptible to fire due to long periods of scarcity.

The area where the PNA is located has a history of rural area abandonment and exodus, resulting in the territories being more vulnerable to the occurrence of wildfires and water scarcity due to an increase in drought times. This scenario, as demonstrated by Kaczan and Orgill-Meyer [49] and Warner et al. [46], points to a tendency for the intensification of migratory processes and environmental degradation due to the territories' lack of resilience to climate change, something dependent on public policies that aid in the establishment of the population in the territories, as long as they have access to infrastructures, public services, and financial resources to develop activities that support their local permanent population.

Consequently, it is important to recognize some of the limitations of this kind of study: (1) Studies on LULC modeling are limited by the scale of the available data; in the present research the COS scale has a scale of 1:25,000, an adequate value for planning actions on a regional-local scale. However, depending on the scale of LULC data available, the results may not be suitable for regional-local planning actions [50]. (2) Using temperature and precipitation data obtained from the WordClim portal, we established an association to comprehend the pattern of change in these variables over periods of 20 years. According to the objectives, future studies can be produced for any period; this must be taken into account when defining the dates of the use and occupation models (LULC) and the database of the climatic variables that will be employed [51,52]. (3) LULC and climate modeling are predictions based on pre-defined models that have been verified in the scientific literature, but which may be contested or replaced as scientific study advances [53,54].

Future research should focus on analyzing the effects of LULC and climate change on the availability of ecosystem services in the PNA, with a focus on ecosystem services related to water supply to emphasize the important role of PA in producing and retaining water as well as regulating surface flow.

5. Conclusions

The main function of a PA is to ensure the long-term functionality of ecosystems by providing ecosystem services such as water supply, carbon storage, and microclimate regulation. The management models for PAs vary across countries, with some allowing

human occupation while others have strict preservation policies that forbid any human activity within the PA boundaries.

Studies [18,35,36,55] frequently employ LULC modeling and prediction. With the Molusce plugin, it is possible to implement this tool at a low cost despite the fact that its use usually requires using commercial software. The results of the LULC modeling can then be examined with the aid of another piece of open-source software (RStudio), which provides the necessary packages for the relationship made between the land use classes and the history and climate trends in the PA, by using the WordClim database that provides the latest CMIP6 data. This analysis validated the LULC modeling, identifying a trend of increased precipitation through the period 2041–2060, which confirms the expansion of forested and bush areas, mainly with the replacement of open areas or non-vegetation. It also shows a stabilization of the artificial surface and a retraction of agricultural activity, with a tendency for these areas to decrease.

Even if the scenario of changes in the LULC can be considered important for the stability of the ecosystems, it must be considered that the climatic data in the subsequent period 2061–2080 indicate an accentuated trend in the decrease of precipitation and an increase in temperatures.

According to studies [56–58], the Iberian Peninsula will be experiencing a 10–15% decrease in precipitation by the end of the twenty-first century, with an increase in the intensity and frequency of extreme precipitation concentrated in winter. Changes in precipitation variability and extreme events were previously investigated on the Iberian Peninsula over the last 50 years of the twentieth century and the early decades of the twenty-first century [59–61]. These scenarios can accentuate the occurrence of extreme events such as wildfires and increase the period of water scarcity [62,63].

Supplementary Materials: The following supporting information can be downloaded at: <https://www.mdpi.com/article/10.3390/land12071302/s1>, Figure S1: Histogram precipitation data; Table S1: Precipitation data statistic; Figure S2: Histogram temperature data (RCP 4.5); Table S2: Temperature data statistic (RCP 4.5); Figure S3: Histogram temperature data (RCP 8.5); Table S3: Temperature data statistic (RCP 8.5); Table S4: Mean month precipitation in PNA (HadGEM3-GC31-LL, RCP 4.5); Table S5: Mean month precipitation in PNA (HadGEM3-GC31-LL, RCP 8.5); Table S6: Mean month minimum temperature in PNA (HadGEM3-GC31-LL, RCP 4.5); Table S7: Mean month minimum temperature in PNA (HadGEM3-GC31-LL, RCP 8.5); Table S8: Mean month maximum temperature in PNA (HadGEM3-GC31-LL, RCP 4.5); Table S9: Mean month maximum temperature in PNA (HadGEM3-GC31-LL, RCP 8.5); Table S10: Precipitation by land use classes (RCP 4.5); Table S11: Precipitation by land use classes (RCP 8.5); Table S12: Minimum temperature by land use classes (RCP 4.5); Table S13: Minimum temperature by land use classes (RCP 8.5); Table S14: Maximum temperature by land use classes (RCP 4.5); Table S15: Maximum temperature by land use classes (RCP 8.5).

Author Contributions: Conceptualization, S.F.; methodology, software, validation, and formal analysis, S.F.; investigation; resources, S.F., A.V., A.B.-G., S.S., T.M. and J.N.; data curation and writing—original draft preparation, S.F.; writing—review and editing, A.V. and A.B.-G.; visualization and supervision, A.V. and A.B.-G.; project administration, A.V.; funding acquisition, A.V. All authors have read and agreed to the published version of the manuscript.

Funding: This research was funded by the European Regional Development Fund. Climate Change Resilient Tourism in Protected Areas of Northern Portugal (CLICTOUR-Project NORTE-01-0145-FEDER-000079).

Data Availability Statement: Portugal land use dataset, available at: <https://snig.dgterritorio.gov.pt/> (accessed on 15 February 2023). Climate data (historical and projection), available at: <https://www.worldclim.org/> (accessed on 15 February 2023).

Conflicts of Interest: The authors declare no conflict of interest.

References

1. UN. *The Millennium Development Goals Report*; UN: New York, NY, USA, 2015.
2. Sobhani, P.; Esmaeilzadeh, H.; Barghjelveh, S.; Sadeghi, S.M.M.; Marcu, M.V. Habitat Integrity in Protected Areas Threatened by LULC Changes and Fragmentation: A Case Study in Tehran Province, Iran. *Land* **2021**, *11*, 6. [[CrossRef](#)]
3. Ervin, J.; Sekhran, N.; Gidda, S.; Vergeichik, M.; Mee, J. *PAs for the 21st Century: Lessons from UNDP/GEF's Portfolio*; UNDP: New York, NY, USA, 2010.
4. Watson, J.E.M.; Dudley, N.; Segan, D.B.; Hockings, M. The Performance and Potential of Protected Areas. *Nature* **2014**, *515*, 67–73. [[CrossRef](#)] [[PubMed](#)]
5. Convention on Biological Diversity. *COP 10 Decision X/2: Strategic Plan for Biodiversity 2011–2020*; Convention on Biological Diversity: Montreal, QC, Canada, 2010.
6. Melillo, J.M.; Lu, X.; Kicklighter, D.W.; Reilly, J.M.; Cai, Y.; Sokolov, A.P. Protected Areas' Role in Climate-Change Mitigation. *Ambio* **2016**, *45*, 133–145. [[CrossRef](#)]
7. Silva, R.M.d.; Lopes, A.G.; Santos, C.A.G. Deforestation and Fires in the Brazilian Amazon from 2001 to 2020: Impacts on Rainfall Variability and Land Surface Temperature. *J. Environ. Manag.* **2023**, *326*, 116664. [[CrossRef](#)] [[PubMed](#)]
8. Folharini, S.d.O.; de Melo, S.N.; Cameron, S.R. Effect of Protected Areas on Forest Crimes in Brazil. *J. Environ. Plan. Manag.* **2022**, *65*, 272–287. [[CrossRef](#)]
9. da Silva, R.F.B.; de Castro Victoria, D.; Nossack, F.Á.; Viña, A.; Millington, J.D.A.; Vieira, S.A.; Batistella, M.; Moran, E.; Liu, J. Slow-down of Deforestation Following a Brazilian Forest Policy Was Less Effective on Private Lands than in All Conservation Areas. *Commun. Earth Environ.* **2023**, *4*, 111. [[CrossRef](#)]
10. Kleemann, J.; Zamora, C.; Villacis-Chiluisa, A.B.; Cuenca, P.; Koo, H.; Noh, J.K.; Fürst, C.; Thiel, M. Deforestation in Continental Ecuador with a Focus on Protected Areas. *Land* **2022**, *11*, 268. [[CrossRef](#)]
11. Dietz, J.; Treydte, A.C.; Lippe, M. Exploring the Future of Kafue National Park, Zambia: Scenario-Based Land Use and Land Cover Modelling to Understand Drivers and Impacts of Deforestation. *Land Use Policy* **2023**, *126*, 106535. [[CrossRef](#)]
12. Yangouliba, G.I.; Zoungrana, B.J.-B.; Hackman, K.O.; Koch, H.; Liersch, S.; Sintondji, L.O.; Dipama, J.-M.; Kwawuvi, D.; Ouedraogo, V.; Yabré, S.; et al. Modelling Past and Future Land Use and Land Cover Dynamics in the Nakambe River Basin, West Africa. *Model. Earth Syst. Environ.* **2022**, *9*, 1651–1667. [[CrossRef](#)]
13. Mingarro, M.; Lobo, J.M. European National Parks Protect Their Surroundings but Not Everywhere: A Study Using Land Use/Land Cover Dynamics Derived from CORINE Land Cover Data. *Land Use Policy* **2023**, *124*, 106434. [[CrossRef](#)]
14. Kubacka, M.; Żywica, P.; Vila Subirós, J.; Bródka, S.; Macias, A. How Do the Surrounding Areas of National Parks Work in the Context of Landscape Fragmentation? A Case Study of 159 Protected Areas Selected in 11 EU Countries. *Land Use Policy* **2022**, *113*, 105910. [[CrossRef](#)]
15. Sohl, T.L.; Claggett, P.R. Clarity versus Complexity: Land-Use Modeling as a Practical Tool for Decision-Makers. *J. Environ. Manag.* **2013**, *129*, 235–243. [[CrossRef](#)]
16. Halmy, M.W.A.; Gessler, P.E.; Hicke, J.A.; Salem, B.B. Land Use/Land Cover Change Detection and Prediction in the North-Western Coastal Desert of Egypt Using Markov-CA. *Appl. Geogr.* **2015**, *63*, 101–112. [[CrossRef](#)]
17. Manandhar, R.; Odeh, I.; Ancev, T. Improving the Accuracy of Land Use and Land Cover Classification of Landsat Data Using Post-Classification Enhancement. *Remote Sens.* **2009**, *1*, 330–344. [[CrossRef](#)]
18. Singh, S.K.; Mustak, S.; Srivastava, P.K.; Szabó, S.; Islam, T. Predicting Spatial and Decadal LULC Changes Through Cellular Automata Markov Chain Models Using Earth Observation Datasets and Geo-Information. *Environ. Process.* **2015**, *2*, 61–78. [[CrossRef](#)]
19. Lantman, J.v.S.; Verburg, P.H.; Bregt, A.; Geertman, S. Core Principles and Concepts in Land-Use Modelling: A Literature Review. In *Land-Use Modelling in Planning Practice*; Koomen, E., Borsboom-van Beurden, J., Eds.; GeoJournal Library, Springer: Berlin/Heidelberg, Germany, 2011; Volume 101, pp. 35–57. ISBN 978-94-007-1821-0.
20. Kindu, M.; Schneider, T.; Teketay, D.; Knoke, T. Changes of Ecosystem Service Values in Response to Land Use/Land Cover Dynamics in Munessa–Shashemene Landscape of the Ethiopian Highlands. *Sci. Total Environ.* **2016**, *547*, 137–147. [[CrossRef](#)] [[PubMed](#)]
21. Nelson, E.; Sander, H.; Hawthorne, P.; Conte, M.; Ennaanay, D.; Wolny, S.; Manson, S.; Polasky, S. Projecting Global Land-Use Change and Its Effect on Ecosystem Service Provision and Biodiversity with Simple Models. *PLoS ONE* **2010**, *5*, e14327. [[CrossRef](#)]
22. Fick, S.E.; Hijmans, R.J. WorldClim 2: New 1-km Spatial Resolution Climate Surfaces for Global Land Areas. *Int. J. Climatol.* **2017**, *37*, 4302–4315. [[CrossRef](#)]
23. Panagos, P.; Ballabio, C.; Meusburger, K.; Spinoni, J.; Alewell, C.; Borrelli, P. Towards Estimates of Future Rainfall Erosivity in Europe Based on REDES and WorldClim Datasets. *J. Hydrol.* **2017**, *548*, 251–262. [[CrossRef](#)] [[PubMed](#)]
24. Pan, Z.; He, J.; Liu, D.; Wang, J. Predicting the Joint Effects of Future Climate and Land Use Change on Ecosystem Health in the Middle Reaches of the Yangtze River Economic Belt, China. *Appl. Geogr.* **2020**, *124*, 102293. [[CrossRef](#)]
25. Guo, M.; Ma, S.; Wang, L.-J.; Lin, C. Impacts of Future Climate Change and Different Management Scenarios on Water-Related Ecosystem Services: A Case Study in the Jianghuai Ecological Economic Zone, China. *Ecol. Indic.* **2021**, *127*, 107732. [[CrossRef](#)]
26. Hürlimann, M.; Guo, Z.; Puig-Polo, C.; Medina, V. Impacts of Future Climate and Land Cover Changes on Landslide Susceptibility: Regional Scale Modelling in the Val d'Aran Region (Pyrenees, Spain). *Landslides* **2022**, *19*, 99–118. [[CrossRef](#)]

27. Andrews, M.B.; Ridley, J.K.; Wood, R.A.; Andrews, T.; Blockley, E.W.; Booth, B.; Burke, E.; Dittus, A.J.; Florek, P.; Gray, L.J.; et al. Historical Simulations with HadGEM3-GC3.1 for CMIP6. *J. Adv. Model. Earth Syst.* **2020**, *12*, 919–933. [[CrossRef](#)]
28. Buck, O.; Niyogi, D.K.; Townsend, C.R. Scale-Dependence of Land Use Effects on Water Quality of Streams in Agricultural Catchments. *Environ. Pollut.* **2004**, *130*, 287–299. [[CrossRef](#)] [[PubMed](#)]
29. Yu, S.; Xu, Z.; Wu, W.; Zuo, D. Effect of Land Use Types on Stream Water Quality under Seasonal Variation and Topographic Characteristics in the Wei River Basin, China. *Ecol. Indic.* **2016**, *60*, 202–212. [[CrossRef](#)]
30. Wang, G.; Xu, Z.; Zhang, S. The Influence of Land Use Patterns on Water Quality at Multiple Spatial Scales in a River System. *Hydrol. Process.* **2014**, *28*, 5259–5272. [[CrossRef](#)]
31. Pijanowski, B.C.; Brown, D.G.; Shellito, B.A.; Manik, G.A. Using Neural Networks and GIS to Forecast Land Use Changes: A Land Transformation Model. *Comput. Environ. Urban Syst.* **2002**, *26*, 553–575. [[CrossRef](#)]
32. Silva, L.P.E.; Xavier, A.P.C.; da Silva, R.M.; Santos, C.A.G. Modeling Land Cover Change Based on an Artificial Neural Network for a Semiarid River Basin in Northeastern Brazil. *Glob. Ecol. Conserv.* **2020**, *21*, e00811. [[CrossRef](#)]
33. Nasiri, V.; Darvishsefat, A.A.; Rafiee, R.; Shirvany, A.; Hemat, M.A. Land Use Change Modeling through an Integrated Multi-Layer Perceptron Neural Network and Markov Chain Analysis (Case Study: Arasbaran Region, Iran). *J. For. Res.* **2019**, *30*, 943–957. [[CrossRef](#)]
34. Isik, S.; Kalin, L.; Schoonover, J.E.; Srivastava, P.; Graeme Lockaby, B. Modeling Effects of Changing Land Use/Cover on Daily Streamflow: An Artificial Neural Network and Curve Number Based Hybrid Approach. *J. Hydrol.* **2013**, *485*, 103–112. [[CrossRef](#)]
35. Folharini, S.; Oliveira, R. Utilização Do Land Change Modeler® Na Modelação Prospetiva Do Uso e Cobertura Do Solo Na Microrregião de Santos, Brasil Para o Ano de 2022. *GOT J. Geogr. Spat. Plan.* **2020**, *19*, 57–73. [[CrossRef](#)]
36. Abbas, Z.; Yang, G.; Zhong, Y.; Zhao, Y. Spatiotemporal Change Analysis and Future Scenario of LULC Using the CA-ANN Approach: A Case Study of the Greater Bay Area, China. *Land* **2021**, *10*, 584. [[CrossRef](#)]
37. Saputra, M.H.; Lee, H.S. Prediction of Land Use and Land Cover Changes for North Sumatra, Indonesia, Using an Artificial-Neural-Network-Based Cellular Automaton. *Sustainability* **2019**, *11*, 3024. [[CrossRef](#)]
38. Tolentino, F.M.; de Lourdes Bueno Trindade Galo, M. Selecting Features for LULC Simultaneous Classification of Ambiguous Classes by Artificial Neural Network. *Remote Sens. Appl. Soc. Environ.* **2021**, *24*, 100616. [[CrossRef](#)]
39. Baig, M.F.; Mustafa, M.R.U.; Baig, I.; Takaijudin, H.B.; Zeshan, M.T. Assessment of Land Use Land Cover Changes and Future Predictions Using CA-ANN Simulation for Selangor, Malaysia. *Water* **2022**, *14*, 402. [[CrossRef](#)]
40. Rahman, M.T.U.; Tabassum, F.; Rasheduzzaman, M.; Saba, H.; Sarkar, L.; Ferdous, J.; Uddin, S.Z.; Zahedul Islam, A.Z.M. Temporal Dynamics of Land Use/Land Cover Change and Its Prediction Using CA-ANN Model for Southwestern Coastal Bangladesh. *Environ. Monit. Assess.* **2017**, *189*, 565. [[CrossRef](#)]
41. Exavier, R.; Zeilhofer, P. OpenLand: Software for Quantitative Analysis and Visualization of Land Use and Cover Change. *R J.* **2020**, *12*, 359. [[CrossRef](#)]
42. Santos, F.D.D.; Miranda, P. *Alterações Climáticas em Portugal. Cenários, Impactos, e Medidas de Adaptação*; Gradiva: Lisboa, Portugal, 2006.
43. Rees, P.; Carrilho, M.-J.; Peixoto, J.; Durham, H.; Kupiszewski, M. *Internal Migration and Regional Population Dynamics in Europe: Portugal Case Study*; University of Leeds: Leeds, UK, 1998.
44. Lewis, J.; Williams, A. Portugal: The Decade of Return. *Geography* **1985**, *70*, 178–182.
45. Calix, T. Territorial Asymmetries and Resilience in Portugal: The Low Density Areas of the Northwest. In *New Cities and Migration: An international Debate*; Bologna, R., Ed.; Dipartimento di Architettura, Università degli Studi di Firenze: Firenze, Italy, 2017.
46. Warner, K.; Hamza, M.; Oliver-Smith, A.; Renaud, F.; Julca, A. Climate Change, Environmental Degradation and Migration. *Nat. Hazards* **2010**, *55*, 689–715. [[CrossRef](#)]
47. Konapala, G.; Mishra, A.K.; Wada, Y.; Mann, M.E. Climate Change Will Affect Global Water Availability through Compounding Changes in Seasonal Precipitation and Evaporation. *Nat. Commun.* **2020**, *11*, 3044. [[CrossRef](#)]
48. Dai, A.; Zhao, T.; Chen, J. Climate Change and Drought: A Precipitation and Evaporation Perspective. *Curr. Clim. Chang. Rep.* **2018**, *4*, 301–312. [[CrossRef](#)]
49. Kaczan, D.J.; Orgill-Meyer, J. The Impact of Climate Change on Migration: A Synthesis of Recent Empirical Insights. *Clim. Chang.* **2020**, *158*, 281–300. [[CrossRef](#)]
50. Verburg, P.H.; Alexander, P.; Evans, T.; Magliocca, N.R.; Malek, Z.; Rounsevell, M.D.; van Vliet, J. Beyond Land Cover Change: Towards a New Generation of Land Use Models. *Curr. Opin. Environ. Sustain.* **2019**, *38*, 77–85. [[CrossRef](#)]
51. Cai, Y.; Guan, K.; Lobell, D.; Potgieter, A.B.; Wang, S.; Peng, J.; Xu, T.; Asseng, S.; Zhang, Y.; You, L.; et al. Integrating Satellite and Climate Data to Predict Wheat Yield in Australia Using Machine Learning Approaches. *Agric. For. Meteorol.* **2019**, *274*, 144–159. [[CrossRef](#)]
52. Bai, Y.; Ochuodho, T.O.; Yang, J. Impact of Land Use and Climate Change on Water-Related Ecosystem Services in Kentucky, USA. *Ecol. Indic.* **2019**, *102*, 51–64. [[CrossRef](#)]
53. Li, X.; Yeh, A.G.-O. Neural-Network-Based Cellular Automata for Simulating Multiple Land Use Changes Using GIS. *Int. J. Geogr. Inf. Sci.* **2002**, *16*, 323–343. [[CrossRef](#)]
54. Majumder, M. Artificial Neural Network. In *Feasibility Model of Solar Energy Plants by ANN and MCDM Techniques*; Springer: Berlin/Heidelberg, Germany, 2015; pp. 49–54.

55. Muhammad, R.; Zhang, W.; Abbas, Z.; Guo, F.; Gwiazdzinski, L. Spatiotemporal Change Analysis and Prediction of Future Land Use and Land Cover Changes Using QGIS Molusce Plugin and Remote Sensing Big Data: A Case Study of Linyi, China. *Land* **2022**, *11*, 419. [[CrossRef](#)]
56. Costa, A.C.; Santos, J.A.; Pinto, J.G. Climate Change Scenarios for Precipitation Extremes in Portugal. *Theor. Appl. Climatol.* **2012**, *108*, 217–234. [[CrossRef](#)]
57. de Lima, M.I.P.; Santo, F.E.; Ramos, A.M.; Trigo, R.M. Trends and Correlations in Annual Extreme Precipitation Indices for Mainland Portugal, 1941–2007. *Theor. Appl. Climatol.* **2015**, *119*, 55–75. [[CrossRef](#)]
58. Pereira, S.C.; Carvalho, D.; Rocha, A. Temperature and Precipitation Extremes over the Iberian Peninsula under Climate Change Scenarios: A Review. *Climate* **2021**, *9*, 139. [[CrossRef](#)]
59. Vicente-Serrano, S.; Trigo, R.; López-Moreno, J.; Liberato, M.; Lorenzo-Lacruz, J.; Beguería, S.; Morán-Tejeda, E.; El Kenawy, A. Extreme Winter Precipitation in the Iberian Peninsula in 2010: Anomalies, Driving Mechanisms and Future Projections. *Clim. Res.* **2011**, *46*, 51–65. [[CrossRef](#)]
60. Andrade, C.; Santos, J.; Pinto, J.; Corte-Real, J. Large-Scale Atmospheric Dynamics of the Wet Winter 2009–2010 and Its Impact on Hydrology in Portugal. *Clim. Res.* **2011**, *46*, 29–41. [[CrossRef](#)]
61. de Lima, M.I.P.; Santo, F.E.; Ramos, A.M.; de Lima, J.L.M.P. Recent Changes in Daily Precipitation and Surface Air Temperature Extremes in Mainland Portugal, in the Period 1941–2007. *Atmos. Res.* **2013**, *127*, 195–209. [[CrossRef](#)]
62. Soares, P.M.M.; Lima, D.C.A. Water Scarcity down to Earth Surface in a Mediterranean Climate: The Extreme Future of Soil Moisture in Portugal. *J. Hydrol.* **2022**, *615*, 128731. [[CrossRef](#)]
63. Guerreiro, S.B.; Kilsby, C.G.; Fowler, H.J. Rainfall in Iberian Transnational Basins: A Drier Future for the Douro, Tagus and Guadiana? *Clim. Chang.* **2016**, *135*, 467–480. [[CrossRef](#)]

Disclaimer/Publisher’s Note: The statements, opinions and data contained in all publications are solely those of the individual author(s) and contributor(s) and not of MDPI and/or the editor(s). MDPI and/or the editor(s) disclaim responsibility for any injury to people or property resulting from any ideas, methods, instructions or products referred to in the content.